Figure S1a. The three panels present JIRAM spectrometer coverage for Juno planning period JM0002. Top panel: spectra acquired with an emission angle < 40° and footprint size < 500 km. Central panel: as above, but limited to spectra where radiance at 5 μm / cos (emission angle) > 20 μW/(cm 2 sr μm). These are the cases actually processed by our retrieval code. Bottom panel: sun incidence angle for spectra presented in central panel. JM0002 covers the inbound phase of perijove passage ("PJ") number 1, before 2016-08-26, 10:58 UTC.
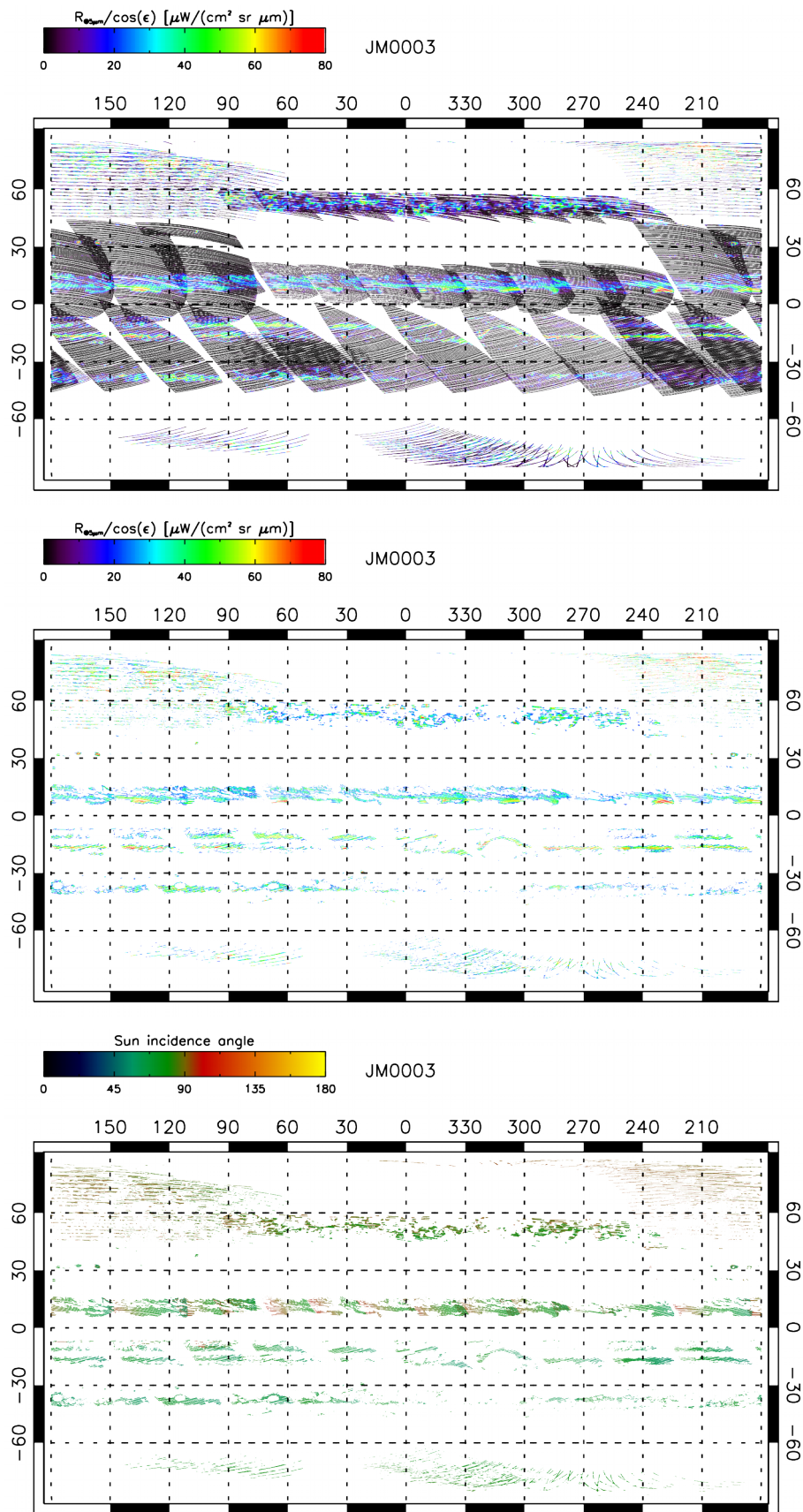
Figure S1b. As S1a, but for Juno planning period JM0003. JM0003 covers the central phase of PJ1, occurred on 2016-08-27.
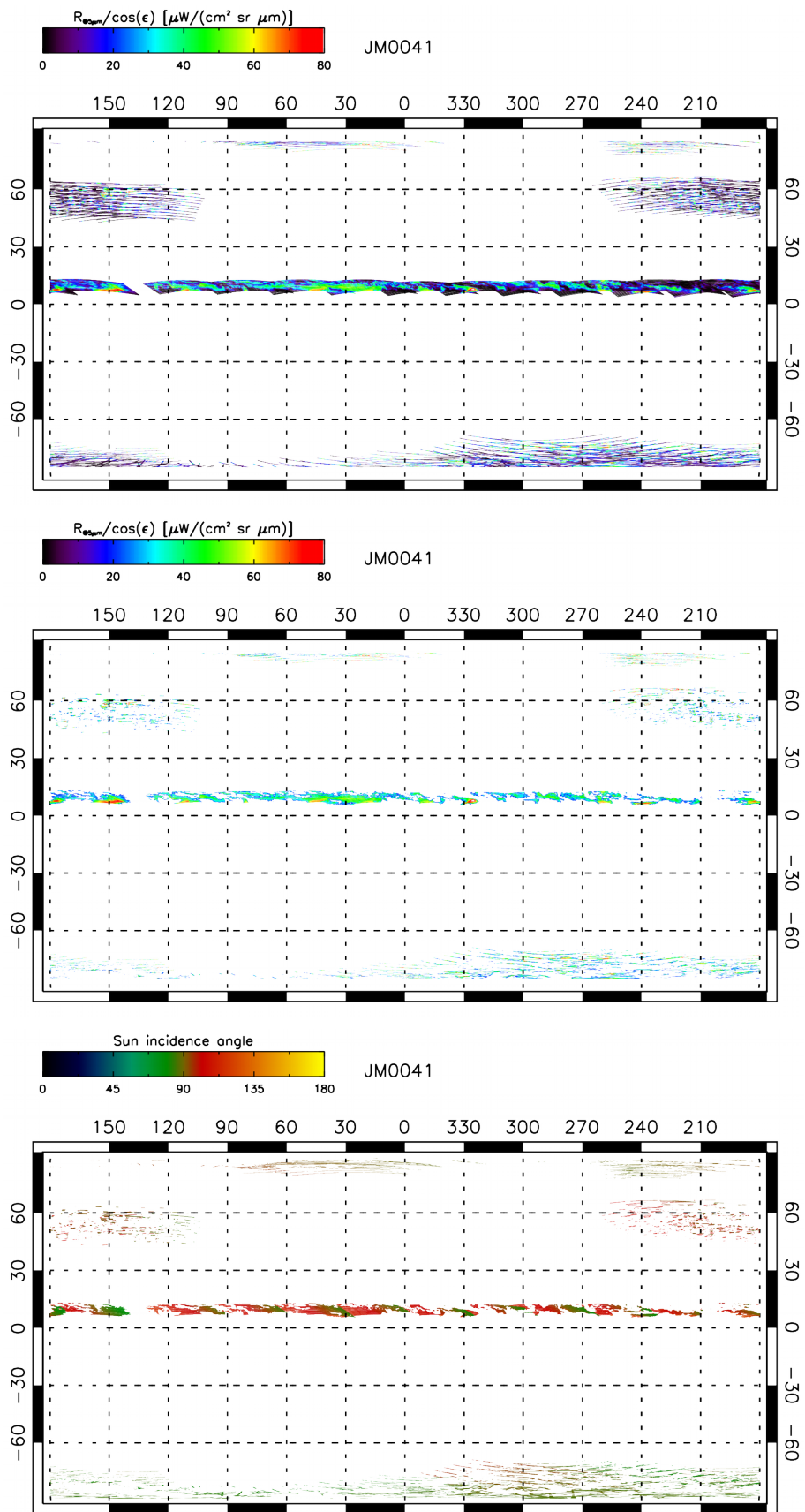
Figure S1c. As S1a, but for Juno planning period JM0041. JM0041 covers the central phase of PJ4, occurred on 2017-02-02.
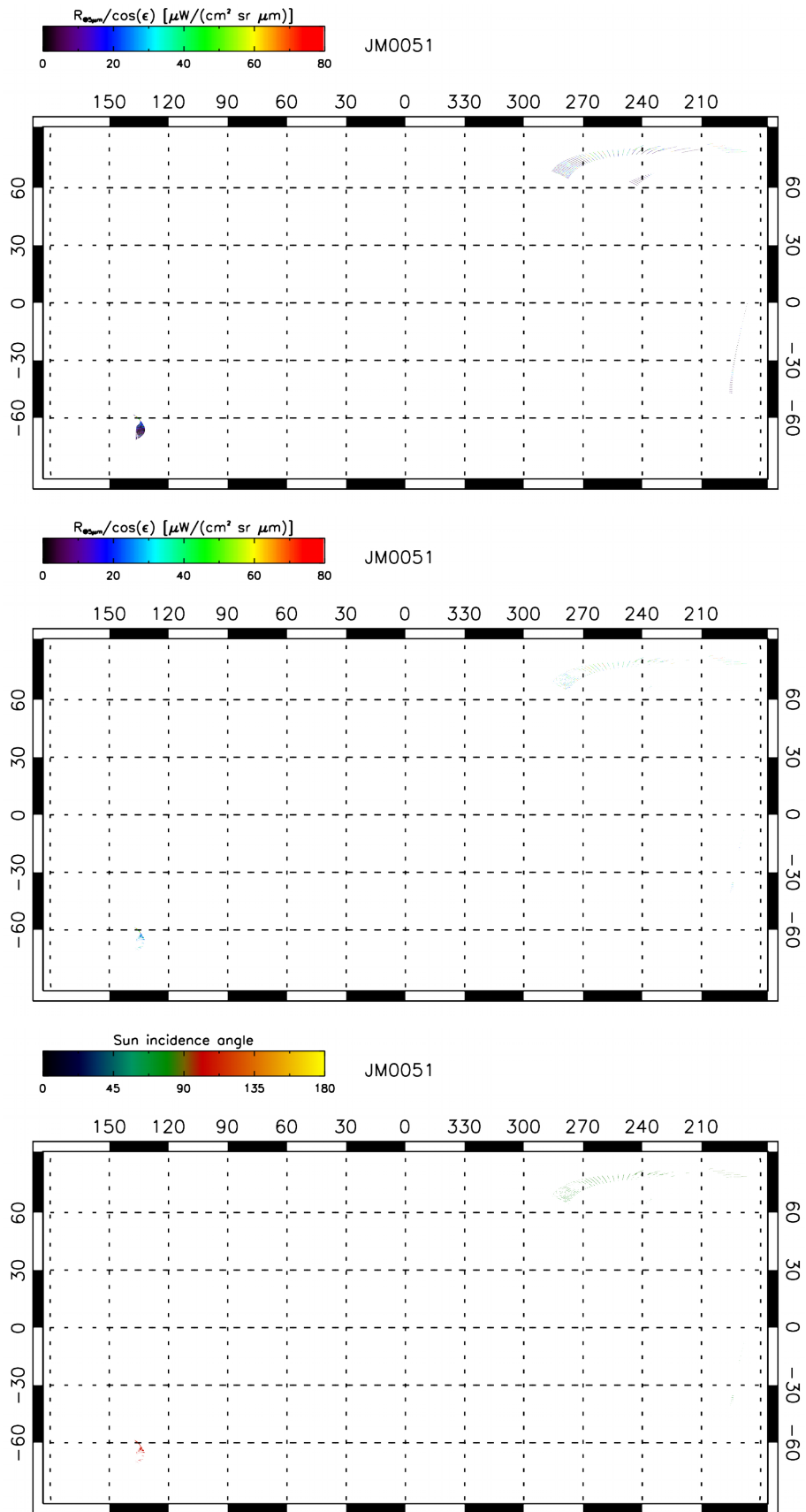
Figure S1d. As S1a, but for Juno planning period JM0051. JM0051 covers the central phase of PJ5, occurred on 2017-03-27.
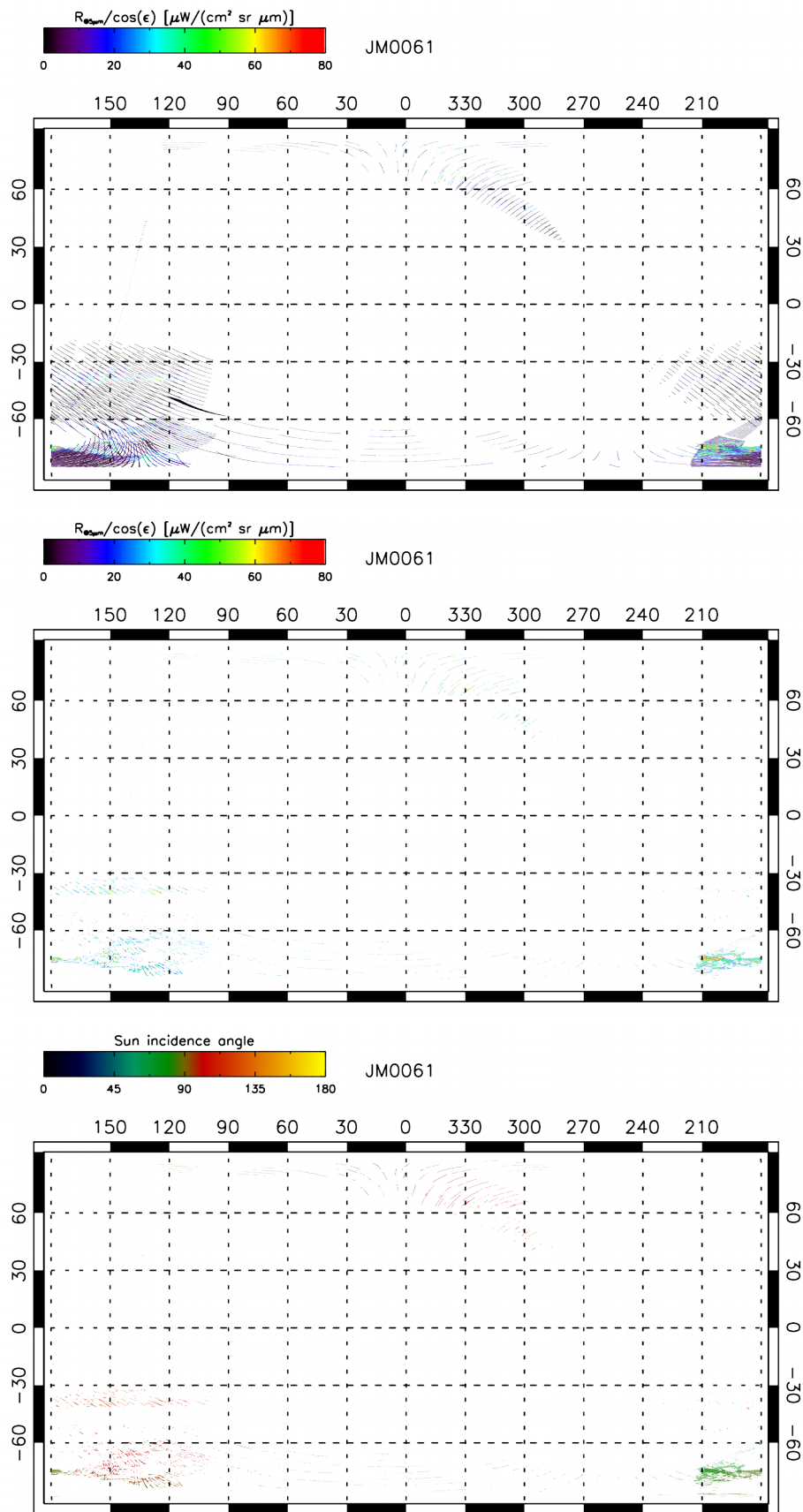
Figure S1e. As S1a, but for Juno planning period JM0061. JM0061 covers the central phase of PJ6, occurred on 2017-05-19.
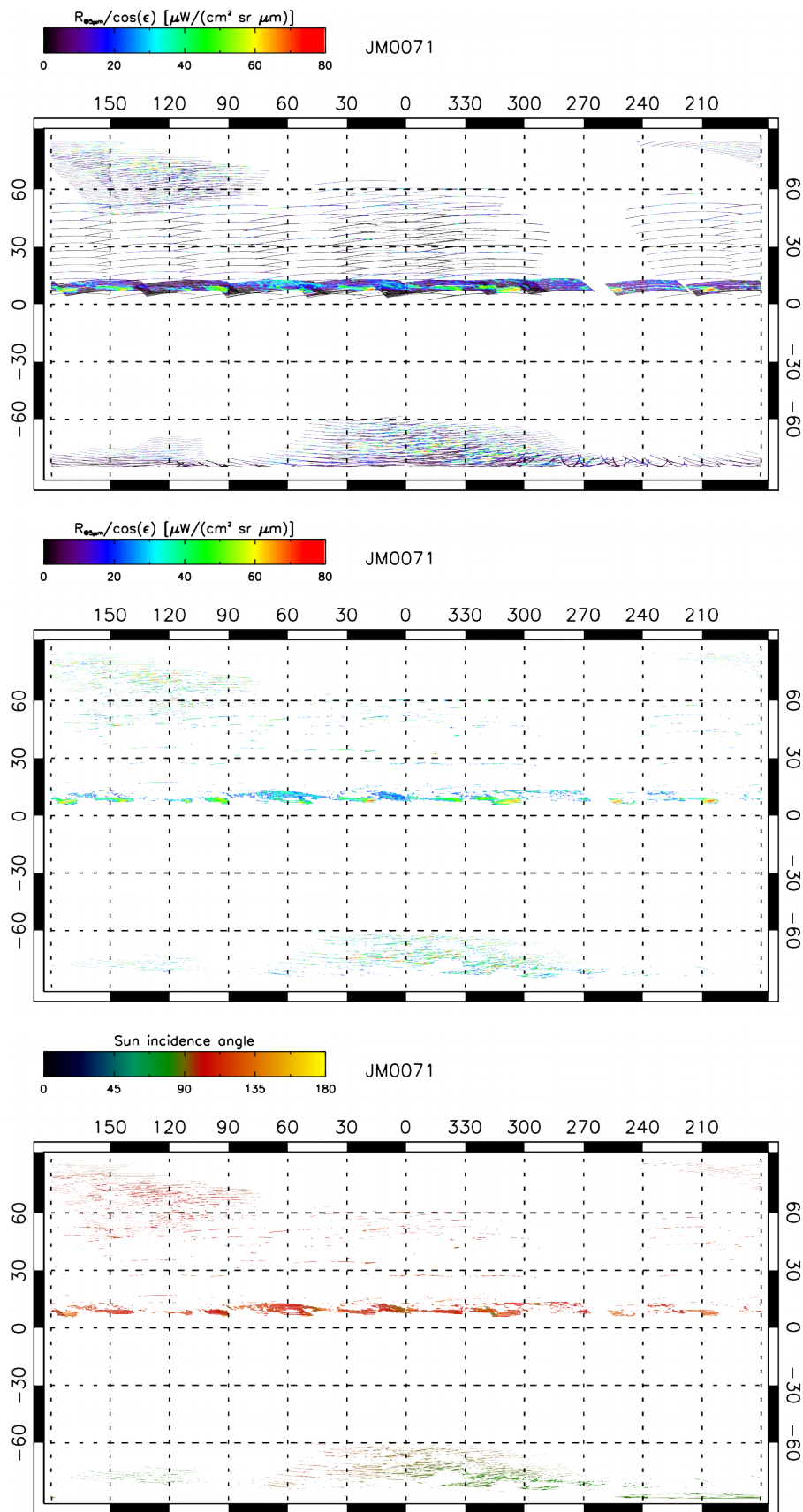
Figure S1f. As S1a, but for Juno planning period JM0071. JM0071 covers the central phase of PJ7, occurred on 2017-07-11.
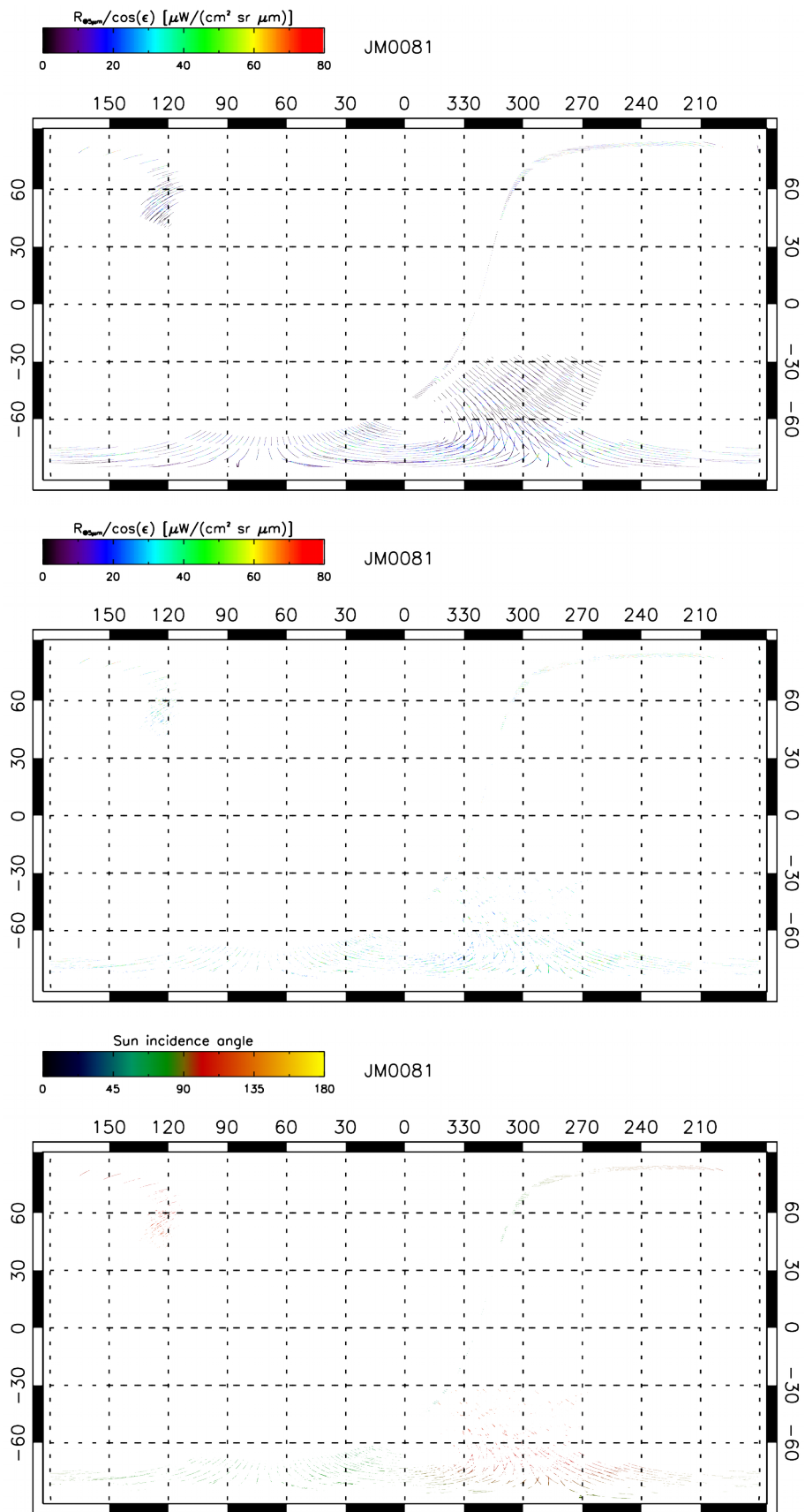
Figure S1g. As S1a, but for Juno planning period JM0081. JM0081 covers the central phase of PJ8, occurred on 2017-09-01.
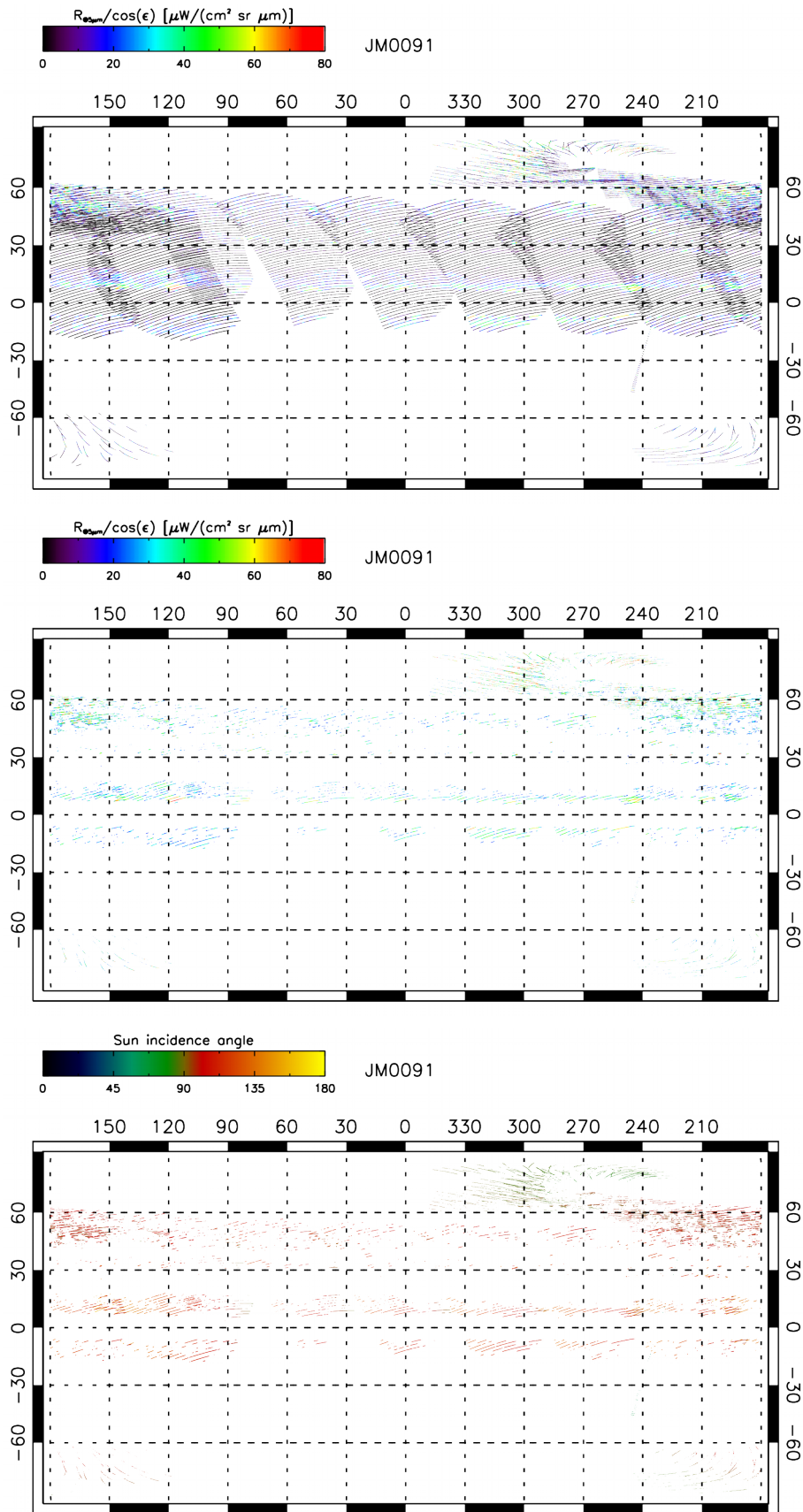
Figure S1h. As S1a, but for Juno planning period JM0091. JM0091 covers the central phase of perijove PJ9, occurred on 2017-10-24.
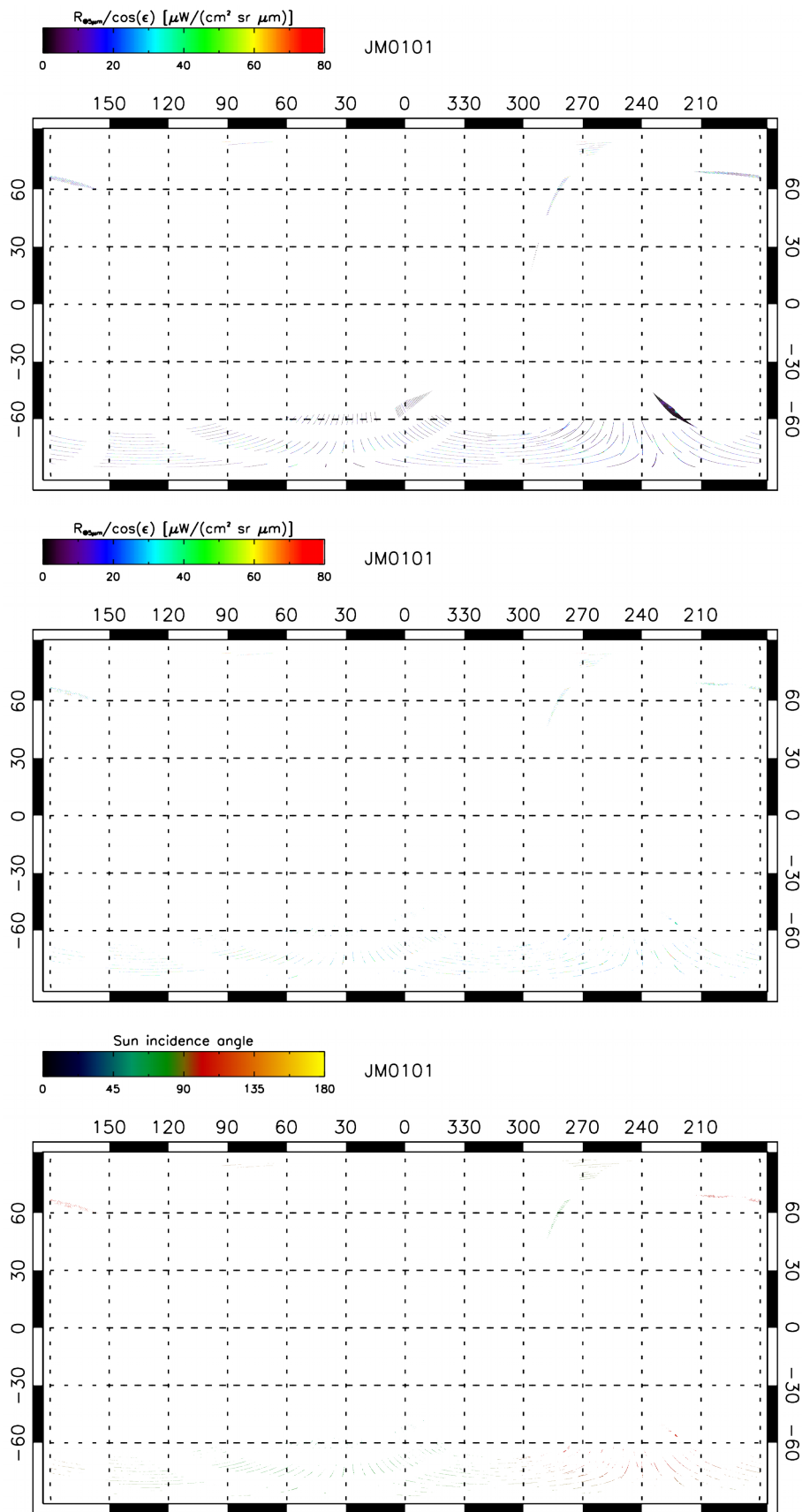
Figure S1i. As S1a, but for Juno planning period JM0101. JM0101 covers the central phase of PJ10, occurred on 2017-12-16.
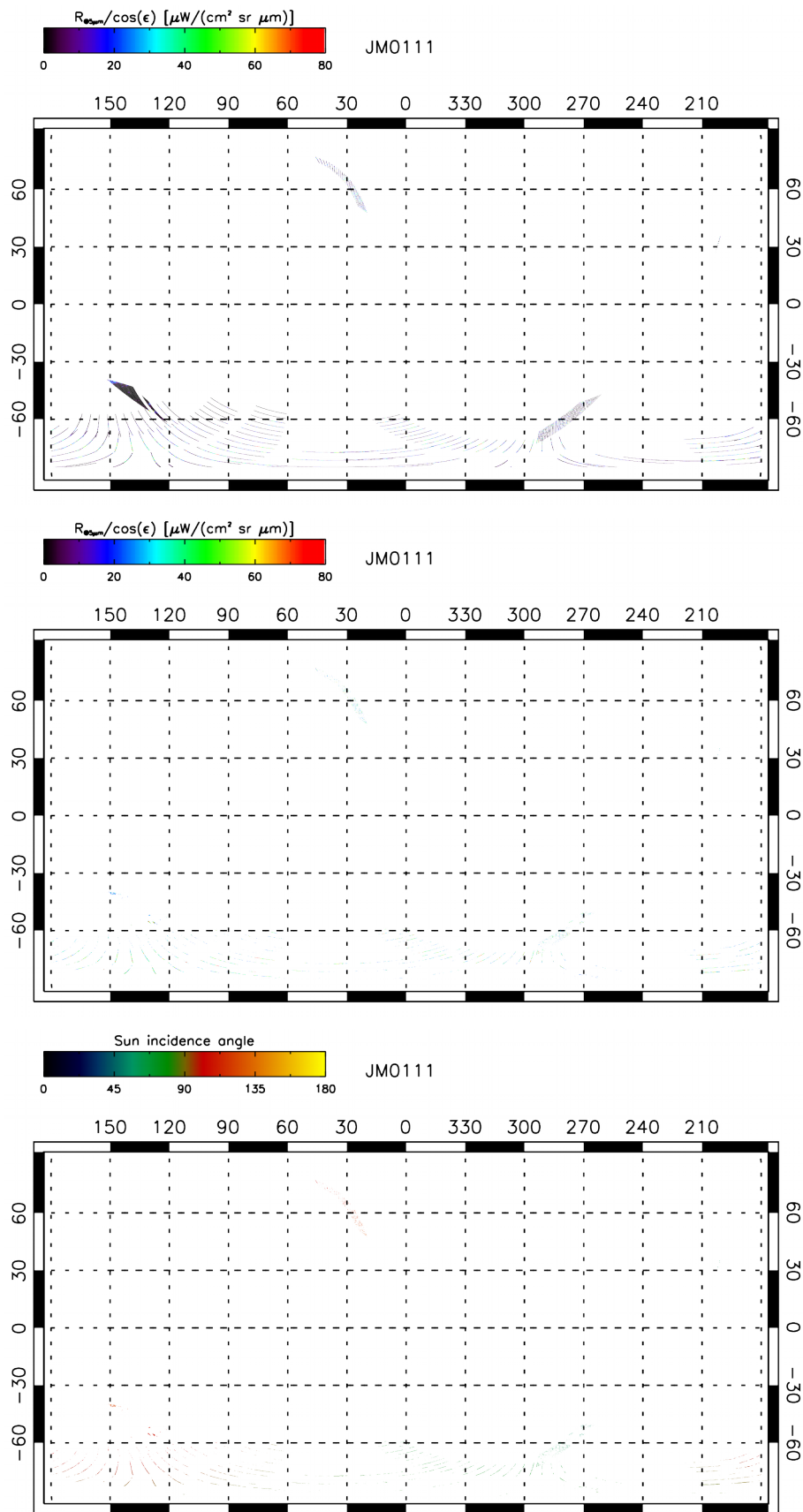
Figure S1j. As S1a, but for Juno planning period JM0111. JM0111 covers the central phase of PJ11, occurred on 2018-02-07.
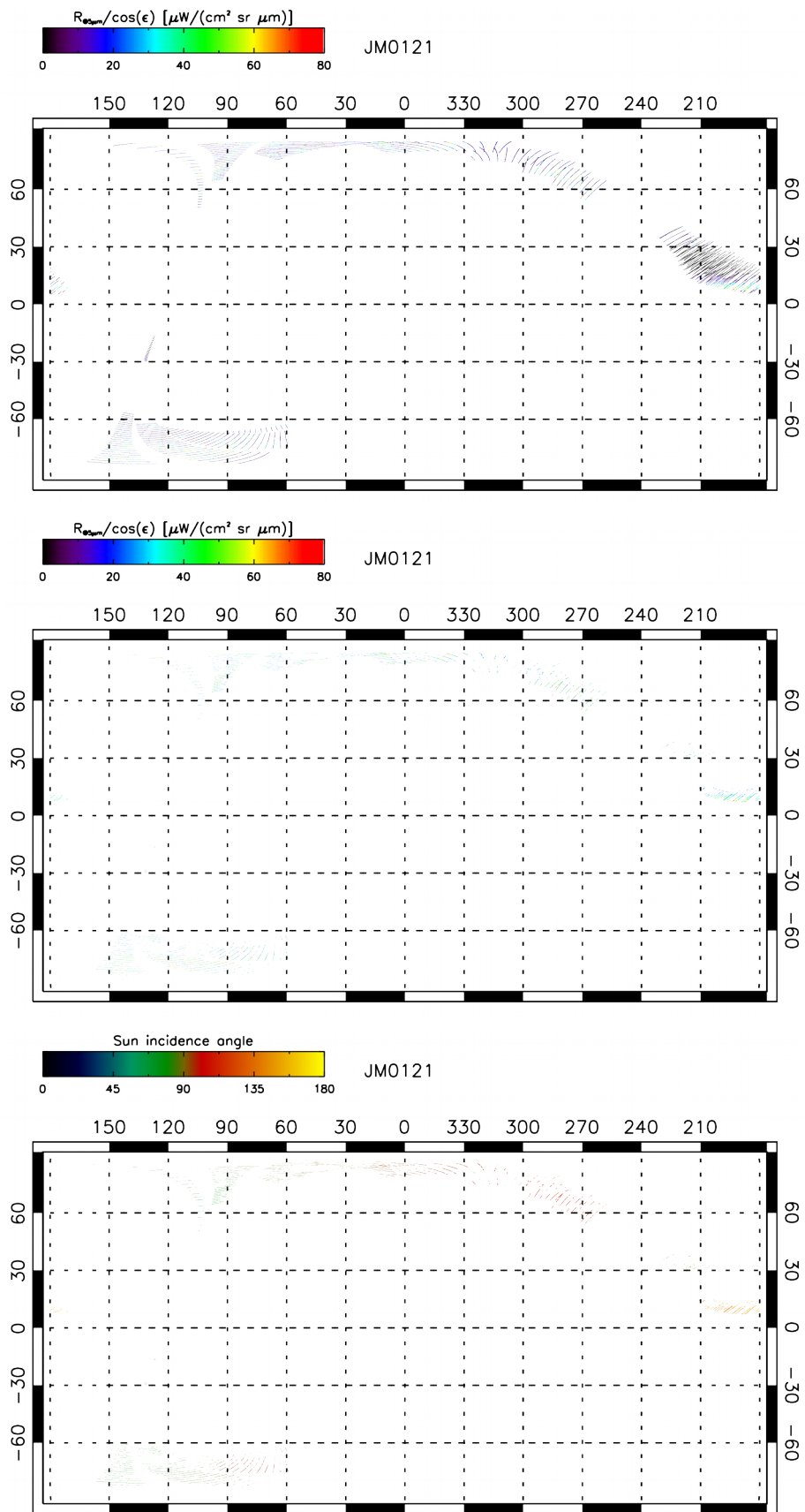
Figure S1k. As S1a, but for Juno planning period JM0121. JM0121 covers the central phase of PJ12, occurred on 2018-04-01.
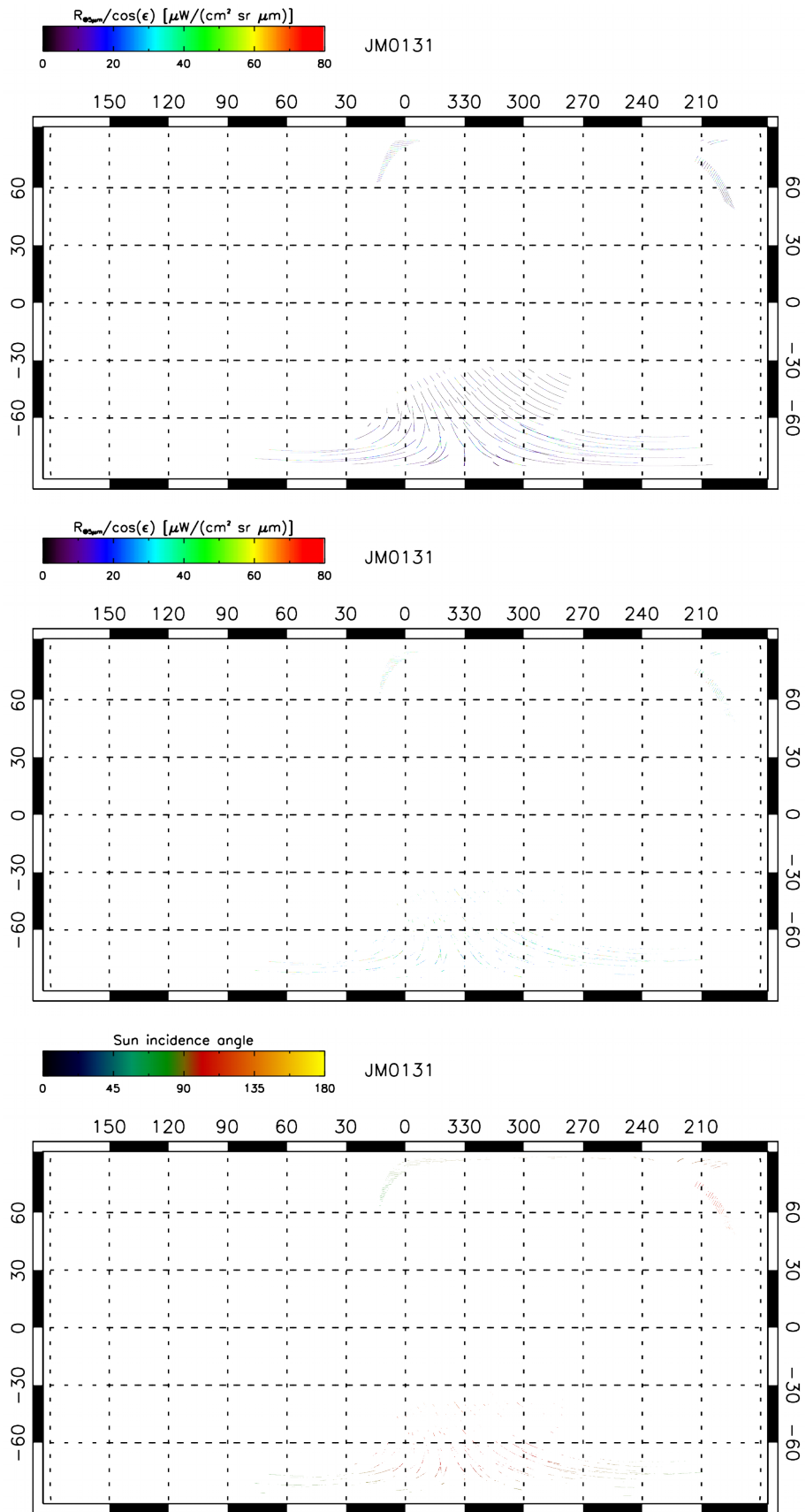
Figure S1l. As S1a, but for Juno planning period JM0131. JM0131 covers the central phase of PJ13, occurred on 2018-05-24.
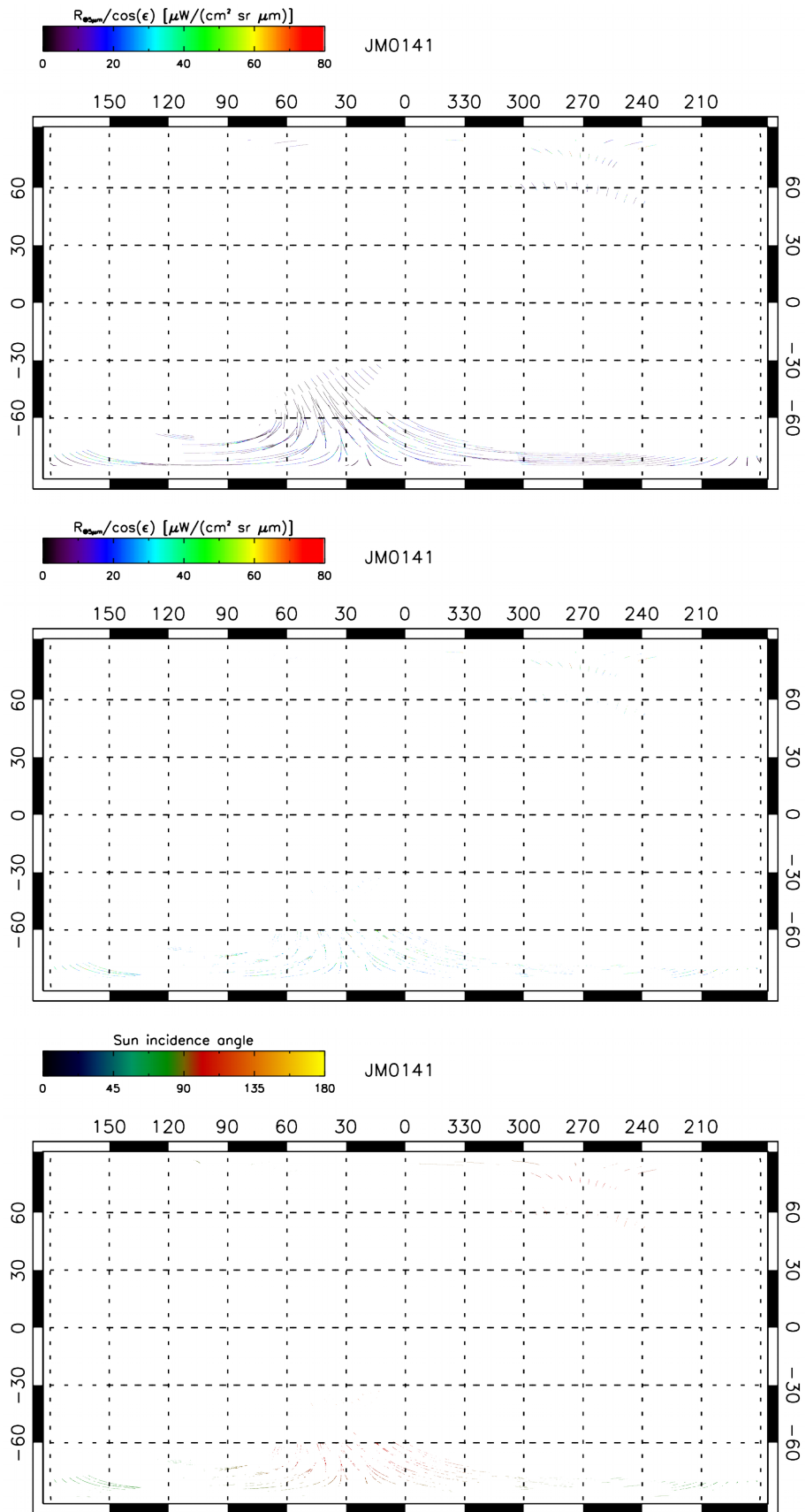
Figure S1m. As S1a, but for Juno planning period JM0141. JM0141 covers the central phase of PJ14, occurred on 2018-07-16.
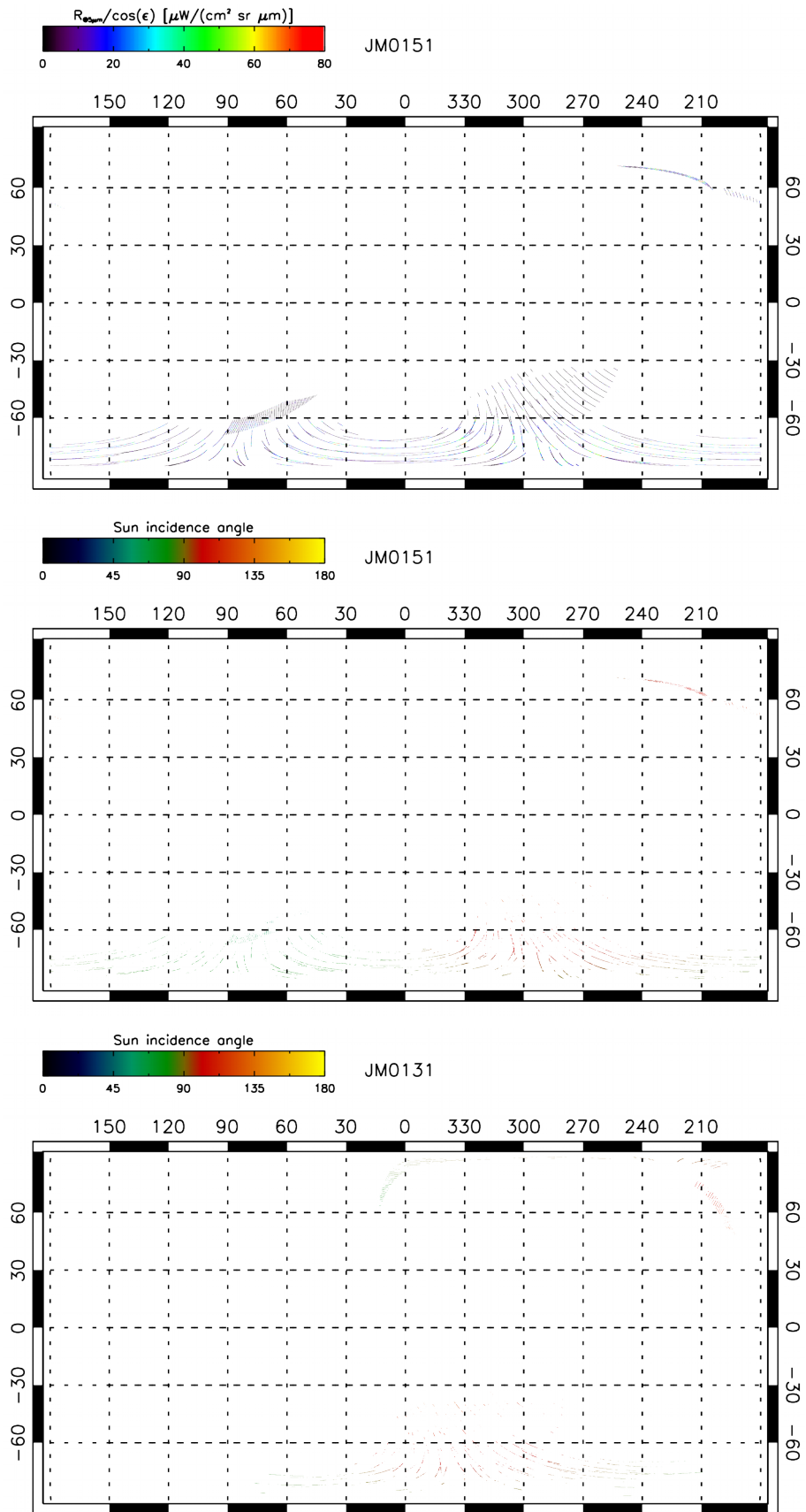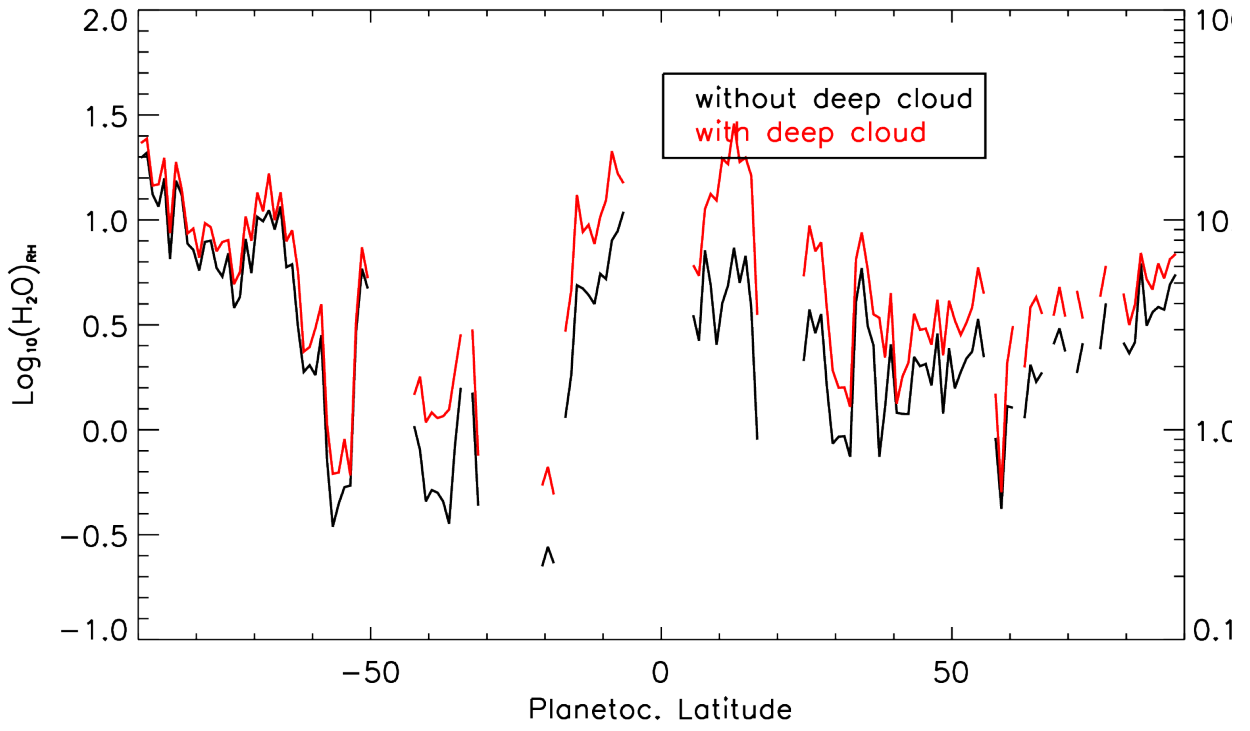
Figure S1n. As S1a, but for Juno planning period JM0151. JM0151 covers the central phase of PJ15, occurred on 2018-09-07.

a
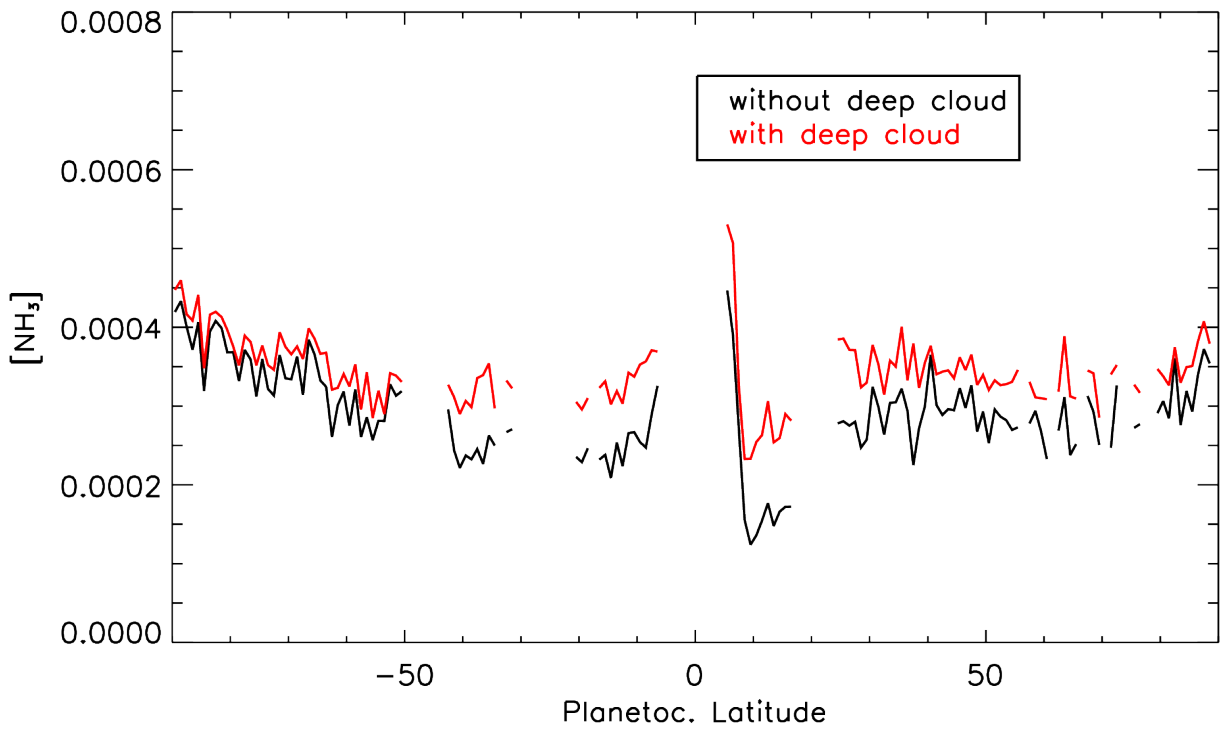
b
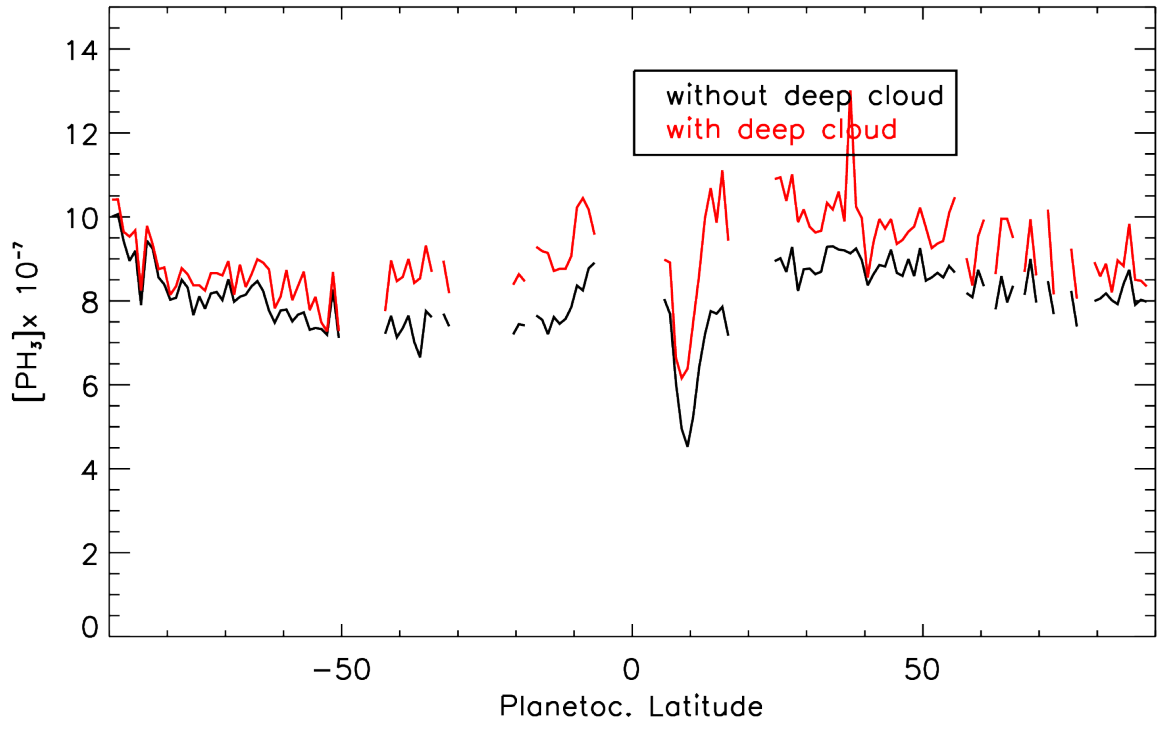
c
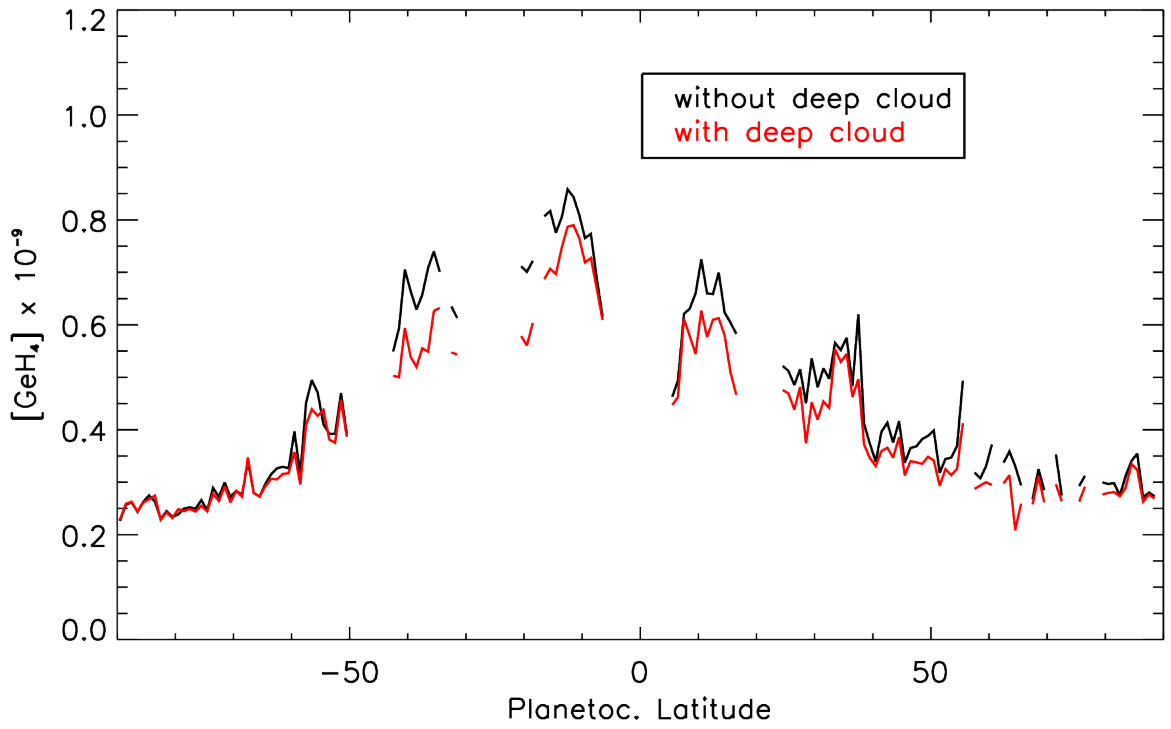
d
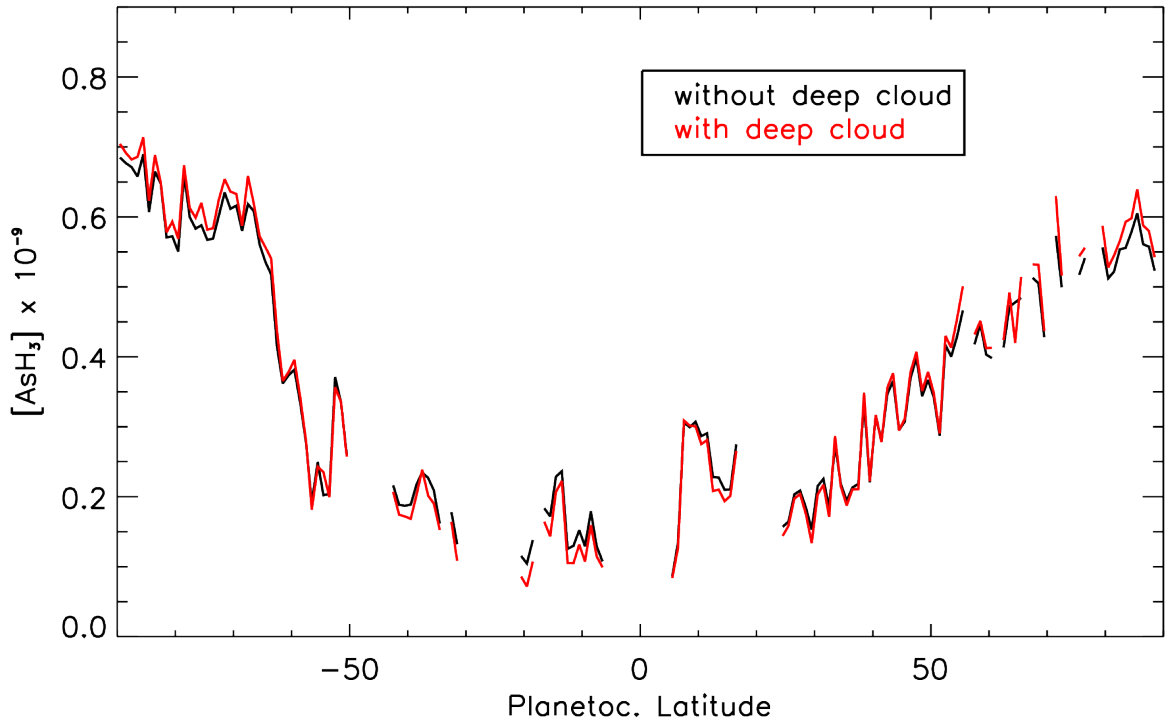
e
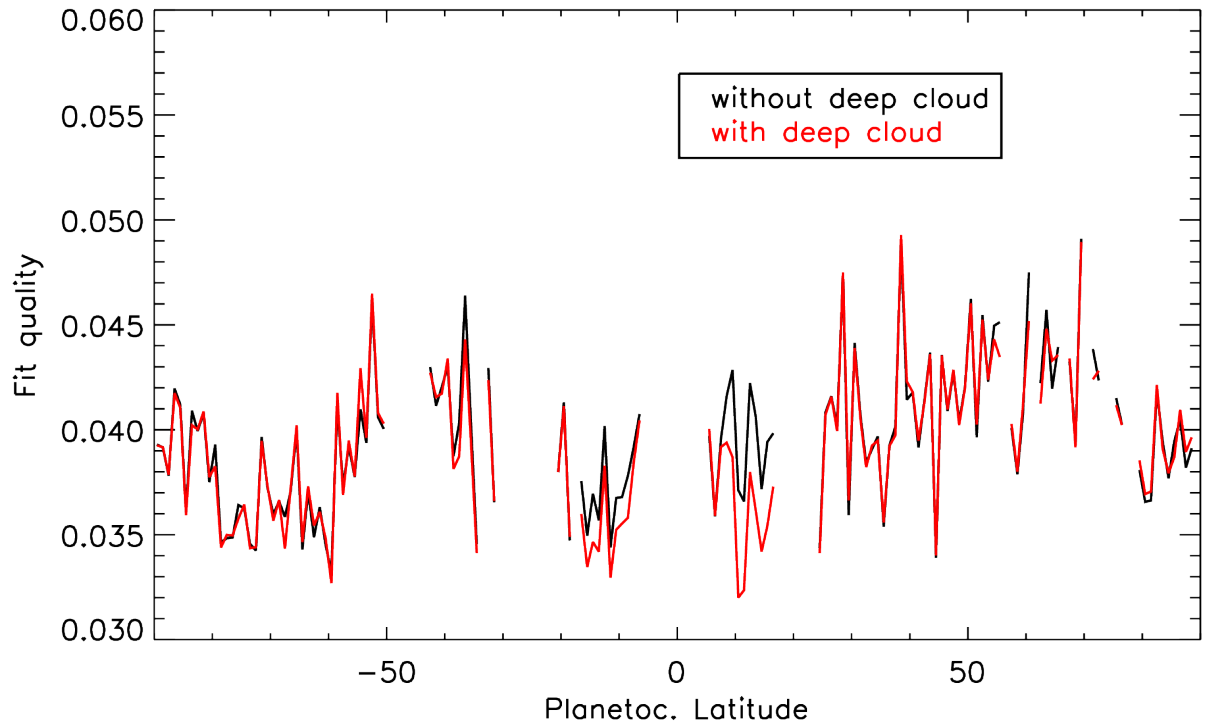
f

Figure S2. Effects of the inclusion of a deep cloud (5bar) on the retrieved latitudinal profiles of gas abundances (a-e) and on fit quality (f). Fit quality here is defined as the average relative difference between the best fit and the observed spectrum in the 4.6-5 μm range. The test was performed on about 10^3 spectra, to be compared against the population of about 3.7×10^5 cases considered in the general discussion.
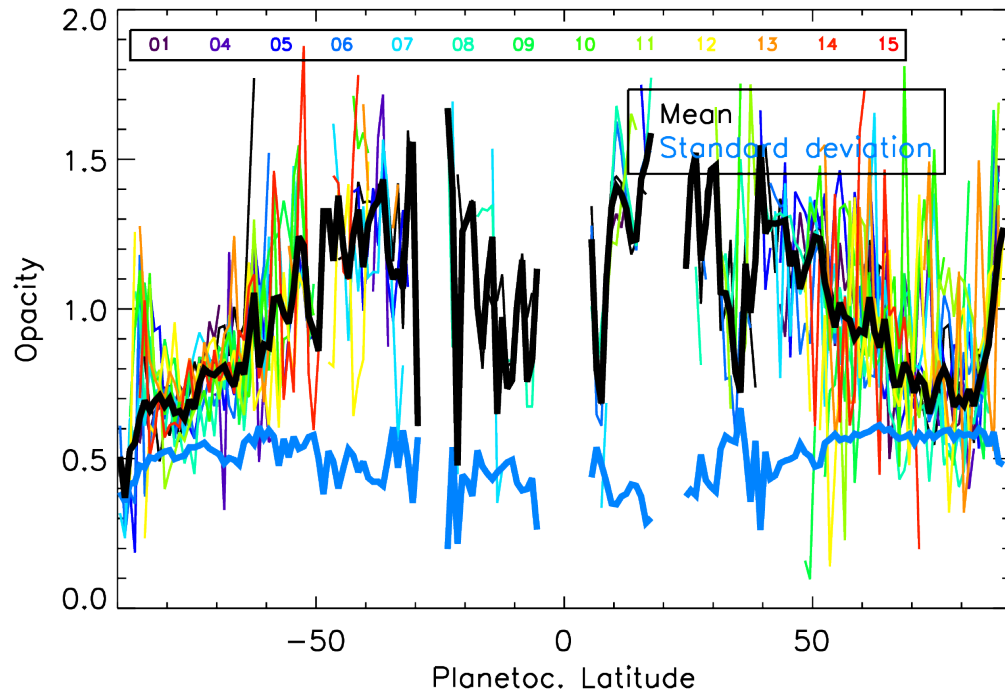
Figure S3. Mean 5-µm opacity of the residual 1-bar cloud in the dataset considered in the study. This plot is severely biased by data filtering described in section 3 and therefore is by no extend representative of global distribution of opacities in the Jupiter atmosphere.

Table I: Comparison of fit qualities achieved removing from free parameters an individual gas and fix it to its a priori value

|	Mean fit quality	Student's t-test		Wilcoxon		cases
		statistic	p	statistic	p	
Reference	3.7%					
H_2O	4.1%	-13.1	$<10^{-6}$	3335	$<10^{-6}$	318
NH_3	4.1%	-17.2	$<10^{-6}$	19378	$<10^{-6}$	535
PH_3	4.8%	-65.2	$<10^{-6}$	182	$<10^{-6}$	638
GeH_4	4.1%	-14.7	$<10^{-6}$	719	$<10^{-6}$	183
AsH_3	4.0%	-17.2	$<10^{-6}$	5945	$<10^{-6}$	377

Table II: Comparison of fit qualities achieved in tests on cloud properties

	Mean fit quality	Student's t-test		Wilcoxon		cases
		statistic	p	statistic	p	
Reference	3.92%					
Deep water cloud	3.89%	3.6	3×10^{-4}	291212	0.3	1099
Reference	3.84%					
Deep water cloud |lat|<20	3.64%	11.8	$<10^{-6}$	2388	$<10^{-6}$	228
Reference	3.94%					
Deep water cloud |lat|>20	3.96%	-1.49	0.13	138629	$<10^{-6}$	871
Reference	3.62%					
Deep water cloud, $[GeH_4]=8\ 10^{-10}$	4.30%	-10.5	$<10^{-6}$	1533	$<10^{-6}$	158
Reference	3.83%					
g=0.8	3.84%	-28.26	$<10^{-6}$	68417	$<10^{-6}$	1768